

Cohesive element model for simulation of crack growth in composite materials

M. Prechtel¹, P. Leiva Ronda², R. Janisch³, G. Leugering¹, A. Hartmaier³, P. Steinmann⁴

¹ Chair of Applied Mathematics II (AM2), Friedrich-Alexander-Universität Erlangen-Nürnberg, Martensstrasse 3, D-91058 Erlangen, Germany, marina.prechtel@am.uni-erlangen.de, leugering@am.uni-erlangen.de

² Chair of General Material Properties (WW1), Friedrich-Alexander-Universität Erlangen-Nürnberg, Martensstrasse 5, D-91058 Erlangen, Germany, Pavel.Leiva-Ronda@ww.uni-erlangen.de

³ Interdisciplinary Centre for Advanced Materials Simulation (ICAMS), Ruhr-Universität Bochum, Stiepeler Straße 129, D-44801 Bochum, Germany, Rebecca.Janisch@rub.de, alexander.hartmaier@rub.de

⁴ Chair of Applied Mechanics (LTM), Friedrich-Alexander-Universität Erlangen-Nürnberg, Egerlandstrasse 5, D-91058 Erlangen, Germany, steinmann@itm.uni-erlangen.de

ABSTRACT. *The fracture energy dissipated by a crack growing in a composite material can be influenced by different material parameters which are affected by the manufacturing process. In case of brittle composite materials, failure mechanisms like debonding of the matrix-fiber interface or fiber breakage can result in crack deflection and hence in the improvement of the damage tolerance of the material. While some material parameters affect dissipative processes during crack growth, others influence the crack path. Concerning simulations of crack growth the cohesive element method provides a framework to model the fracture considering strength, stiffness and failure energy in an integrated manner. Combination with the discontinuous Galerkin method allows to investigate the influence of different cohesive parameters and crack paths on the fracture energy dissipation to optimize the toughness of the considered composite.*

INTRODUCTION

In order to investigate the possibility of influencing crack propagation in composite materials we apply simulation methods which use the concept of cohesive elements that have been introduced in [1] and developed further in [2]. While in these papers crack paths in a fixed domain of a specimen supplied with defined material properties are considered we aim at the simulation of cracks inside different materials of a composite specimen paying attention to various possibilities of cracking processes like fibre debonding and fibre breakage. A good introduction into numerical properties of

cohesive elements and into discretization issues can be found in [3]. Nitsche proposed in [4] a method to enforce Dirichlet boundary conditions in a weak sense. Subsequently, different versions of so called Discontinuous Galerkin (DG) methods have been based on that idea. We take advantage of the use of a DG method as described in [5]. Thereby continuity of the stresses at cohesive elements is enforced without the necessity of questionable determination of penalization parameters for that issue. Following [5] penalization is used for stabilization of the method and for avoiding interpenetration of opposite crack sides. By applying a combination of the FEM with cohesive elements and the DG method, crack paths do not have to be prescribed at the beginning of simulations as done in [2] but rely on a stress criterion. This way varying material parameters and geometrical data of composites may cause different crack paths effecting various amount of energy dissipation. Our objective to maximize the amount of fracture energy for a given load scenario by adjusting material parameters is motivated by studies demonstrating that energy dissipation processes in brittle matrix composites provide toughening of the material. Assuming that homogenization techniques will allow application of the received results to more complicated structures we consider a unit cell of one fibre inside a matrix material.

THEORY AND APPROACH

We consider a bounded domain $\Omega \subset \mathbb{R}^2$ filled with matrix material, where a fibre with rectangular shape is placed inside Ω . The fiber and matrix materials are in general anisotropic. The domain Ω is fixed at the Dirichlet part $\Gamma_D \subset \partial\Omega$ of the boundary $\partial\Omega$ and an external force f is applied to the Neumann part $\Gamma_N \subset \partial\Omega$. We will use the Einstein summation convention for summation over repeated indices in the following. A crack Γ_C is assumed to exist in Ω . There are no volume forces considered, and linear elasticity with displacement field u , strain tensor $e_{kl} = 0.5(u_{k,l} + u_{l,k})$ and stress tensor $\sigma_{ij} = c_{ijkl}e_{kl}$, $i, j, k, l = 1, 2$ is assumed. The elasticity tensor $c_{ijkl} \in L^\infty$, $i, j, k, l = 1, \dots, N$ is symmetric in the sense of $c_{ijkl} = c_{jikl} = c_{klij}$ and fulfills $c_0 \xi_{ij} \xi_{ij} \leq c_{ijkl} \xi_{kl} \xi_{ij} \leq C_0 \xi_{ij} \xi_{ij}$, $c_0, C_0 > 0$.

Cohesive element approach

Processes in the so called cohesive zone around a crack tip play a decisive role for energy dissipation. In [6] an overview to different possibilities of modeling these effects and some material science based overview on different cohesive processes can be found. In our studies we account for the cohesive effects at small crack openings by establishing so called cohesive forces t according to cohesive laws. These laws are characterized by the values of critical stress σ_c , which corresponds to the maximal value of the cohesive force achieved and the critical energy release rate G_c , which corresponds to the area embedded between the curve and the horizontal axis, where the crack opening δ is depicted. As from our point of view the value of G_c is much more important than the specific shape of the curve (see [6] for different possibilities), we

confine our considerations to initially rigid so called UBER (universal binding energy relation [7]) laws with a shape depicted in Figure 1 a). In our studies we pay attention to forces introduced by normal as well as by tangential displacement of opposite crack sides. Therefore we dispose the crack opening δ into its normal part δ_ν and its tangential part δ_τ by $\delta = \delta_\nu \nu + \delta_\tau \tau$ with ν unit vector normal and τ unit vector tangential to the crack surface. According to suitable laws with UBER shape the parts $t_\nu(\delta_\nu)$ and $t_\tau(\delta_\tau)$ can be calculated and the cohesive force for a certain point on the crack is obtained as combination of both parts according to $t = \frac{t_s}{\delta_s} (\beta^2 \delta_\tau \tau + \delta_\nu \nu)$ with $t_s = \sqrt{\beta^{-2} t_\tau^2 + t_\nu^2}$ and $\delta_s = \sqrt{\beta^2 \delta_\tau^2 + \delta_\nu^2}$. Following [8] β is chosen as $\beta = K_{IIc}/K_{Ic}$. For the simulation of cohesive forces in combination with FEM we apply the widely used approach of cohesive elements explained in detail in the mentioned literature. Here we confine ourselves to give a justification of additional terms in the variational formulation of the elasticity problem due to the contribution of cohesive elements. For the sake of simplicity, we confine the consideration to one single cohesive element. This element is placed somewhere in the domain Ω between two continuous elements and a crack may propagate through this element (Figure 1 b)). For a cohesive element two cases may appear. It may stay closed, because a certain criterion for opening is not fulfilled, and therefore no crack path is supposed in that element. In that case it is necessary to enforce continuity of the displacement field $[u] = 0$ and of the stresses $[\sigma]\nu = 0$ at the cohesive element boundary Γ_e where $[\cdot] = (\cdot)|_{\Gamma^+} - (\cdot)|_{\Gamma^-}$ denotes the jump along Γ_e and the normal ν is defined as $\nu := \nu^- = -\nu^+$. The equation $[\sigma]\nu = 0$ can be written as $-\sigma|_{\Gamma_e^+} \nu^+ = \sigma|_{\Gamma_e^-} \nu^-$ so that the integral along Γ_e inside the variational formulation of the elasticity problem with test function v takes the form

$$-\int_{\Gamma_e^+} (\sigma|_{\Gamma_e^+} \nu^+)^T v|_{\Gamma_e^+} da - \int_{\Gamma_e^-} (\sigma|_{\Gamma_e^-} \nu^-)^T v|_{\Gamma_e^-} da = \int_{\Gamma_e} [v]^T v da \quad (1)$$

where the definition $\{\cdot\} := 0.5((\cdot)|_{\Gamma^+} + (\cdot)|_{\Gamma^-})$ is used. If, in the other case, crack development through a cohesive element is supposed and the element is therefore opened, the displacement field becomes discontinuous at Γ_e and cohesive forces $t([u])$ are introduced according to $-\sigma|_{\Gamma_e^+} \nu^+ = \sigma|_{\Gamma_e^-} \nu^- = t([u])$. It is, therefore, obvious that

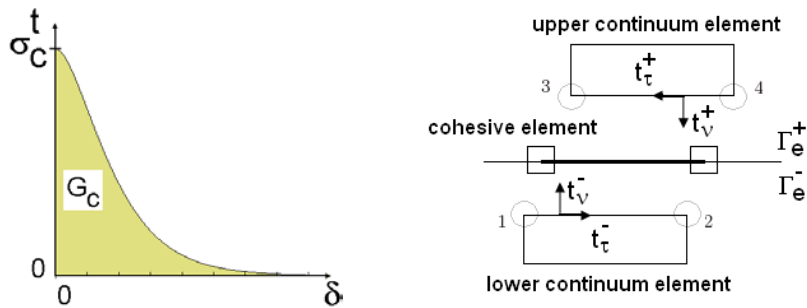


Figure 1. a) Rigid cohesive law

b) Scheme of a cohesive Element

cohesive forces along Γ_e^+ are contrary to cohesive forces along Γ_e^- , which reflects the closing effect of the cohesive forces. Furthermore, it can be deduced that $(\sigma|_{\Gamma_e^+} - \sigma|_{\Gamma_e^-})\nu = 0$ is still fulfilled which shows that the normal part of the stress field is still continuous at Γ_e . Inside the variational formulation the contribution of the cohesive forces appears as

$$-\int_{\Gamma_e^+} (\sigma|_{\Gamma_e^+} \nu^+)^T v|_{\Gamma_e^+} da - \int_{\Gamma_e^-} (\sigma|_{\Gamma_e^-} \nu^-)^T v|_{\Gamma_e^-} da = \int_{\Gamma_e} t([u])^T v da \quad (2)$$

Discontinuous Galerkin method

Regarding the remarks in the last section, it is obvious that the nodes of cohesive elements have to be held together during simulation in the pre-failure regime. As proposed in [5] this can be achieved by applying a type of DG method, which induces a weak enforcement of continuity at the interface by making use of Nitsche's method [4]. The elasticity problem considered in our studies consists in finding $u \in K_0 = \{u \in [H^1(\Omega_0)]^2 : u = 0 \text{ on } \Gamma_D, [u]\nu \geq 0 \text{ on } \Gamma_C\}$ so that the variational formulation $a(u, v) = F(u)$ is fulfilled $\forall v \in K_0$. The equation $a(u, v) = F(u)$ includes the integrals of the variational formulation of the elasticity problem as well as the integrals addressed in the last section and additional integrals stemming from application of the DG method to achieve symmetry of the bilinear form $a(u, v)$ and coercivity of the problem formulation while consistency is guaranteed. Inside the variational formulation some terms concern integrals along cohesive elements as long as they are closed, while others have to be introduced for opened cohesive elements. In order to receive a complete variational formulation including all explained terms, a parameter α is introduced which takes for each cohesive element the value 1 if a crack should propagate through this element and 0 if the element should stay closed. The complete variational formulation for the whole domain Ω with $\Omega_0 = \Omega \setminus \Gamma_C$ then takes the form

$$\begin{aligned} \int_{\Omega_0} c_{ijkl} e_{kl}(u) e_{ij}(v) dx - \int_{\Gamma_C} (1 - \alpha) ([v]^T \{\sigma(u)\} \nu + \nu^T \{\sigma\} [u]) da \\ + \int_{\Gamma_C} [v]^T ((1 - \alpha)\theta[u] + \alpha t([u])) da = \int_{\Gamma_C} f^t v da \end{aligned} \quad (3)$$

The second term in the brackets in the second integral on left hand side of Eq. 3 recovers the symmetry of the bilinear form, while the first term in the third integral on the left hand side ensures the coercivity of the bilinear form for large enough $\theta \in \mathbb{R}$ and, therefore, provides positive definiteness of the corresponding system matrix received after discretization of the problem. See [9] for detailed proofs of this statements. References for the choice of θ can be found in [5]. During simulations the parameter α will be set to 0 or 1 for each cohesive element separately according to the stresses at that element. Thereby the stresses referring to the tangential direction $\sigma_{\tau_e} = |\{\sigma\}_{ij} \nu_j \tau_i|$ and to the normal direction $\sigma_{\nu_e} = \{\sigma\}_{ij} \nu_j \nu_i$ will be taken into account.

Comparing the value $\sigma_{crit} = \sqrt{\beta^{-2}\sigma_{te}^2 + \sigma_{ve}^2}$ with the value of critical stress σ_c given by the cohesive law offers a stress criterion for checking if opening of a cohesive element is indicated.

MAXIMIZATION OF FRACTURE ENERGY

Our aim is to maximize the energy dissipated by a crack, i.e. the so called fracture energy, for a given load scenario. Stresses inside the material inducing crack propagation are due to external loads by boundary forces f or boundary displacements y in our studies. The fracture energy E_d at the end of the simulation is determined as

$$E_d = \int_{\Gamma_c} \int_{\delta=0}^{\delta_{max}} t(\delta) d\delta dr \quad (4)$$

Eq. 4 gives reference to different possibilities for maximizing E_d . Obviously, increasing of E_d can be achieved by adjusting values of the cohesive laws as well as by varying the crack path. In our studies the cohesive parameters for both bulk matrix and fiber have been obtained after a renormalization of first principle (DFT) parameters taking G_c as invariant [10]. Two limiting cases are considered: I. the crack path is completely prescribed, and II. the crack path is completely free.

Studies with prescribed crack paths

In order to compare the influence of different material parameters on the fracture energy for fibre debonding and fibre breakage we start by separately considering two prescribed crack paths as depicted in the models in Figure 2. The matrix material is printed in yellow, the fibre material in blue and the crack path in red. The displacement at the upper boundary is increased during simulation up to a value that at each point on the crack an opening δ_{max} is reached at which the cohesive forces are considered to be zero. As can be seen in Table 1 in case of fibre debonding, increasing the value of G_c^{int} of the interface while keeping σ_c^{int} and the values of the fibre ($G_c^f = 5.7 J/m^2$, $\sigma_c^f = 410MPa$) and matrix ($G_c^m = 2.6 J/m^2$, $\sigma_c^m = 140MPa$) constant increases the

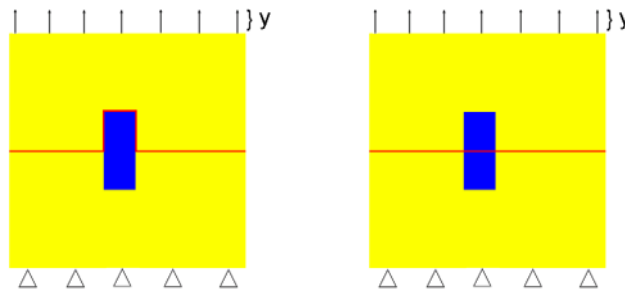


Figure 2. a) Model for fibre debonding b) Model for fibre breakage

value of E_d . Higher values of σ_c^{int} for constant G_c^{int} will also yield higher fracture energy as long as δ_{max} is not yet reached at all points of the crack along the interface, but at the end of the simulation almost the same fracture energy is reached for different values of σ_c^{int} . This can be seen in Figure 3, where on the horizontal axis the vertical displacement y is depicted and on the vertical axis the fracture energy E_d . According to Eq. 4 increasing the crack length also results in higher values of E_d . For the fibre parameters mentioned above and the values $G_c^{int} = 3.5 J/m^2$, $\sigma_c^{int} = 230MPa$ for the interface a crack of the same length inside the fibre will cause higher fracture energy than along the interface. But as can be seen in Table 2 by varying the length width ratio l/b of the fibre and thereby the crack length higher fracture energy is attainable for fibre debonding (E_d^{IF}) than for fibre breakage (E_d^{TF}) for $l/b = 1/3$.

Table 1. Fracture energy for varying G_c^{int} and constant σ_c^{int}

$G_c^{int} (J/m^2)$	2	4	6	10
$E_d (J/m^2)$	2.75	3.56	5.50	6.47

Table 2. Fracture energy for different length/ width ratio (l/b) of the fibre

l/b	12/1	3/1	4/3	3/4	1/3
$E_d^{IF} (J/m^2)$	3.38	3.24	3.29	3.18	3.48
$E_d^{TF} (J/m^2)$	5.00	3.83	3.44	3.25	3.05

Studies with free crack paths

When prescribing crack paths, it has to be kept in mind that the supposed scenario might not be realistic for all considered cohesive parameters, because the stresses in the material make the crack propagate in a different manner. This issue is taken into account if free crack paths instead of prescribed ones are simulated and a stress criterion as explained above is applied. We now consider a load scenario as shown in Figure 2, but with an external force f instead of a displacement y . Instead of the complete prescribed crack paths there is an incipient crack supposed ending before the fibre is reached. The stress distribution introduced by that scenario can be seen in Figure 4 a). An example for a crack path received for a certain load f and with the cohesive values $G_c^m = 4.9 J/m^2$, $\sigma_c^m = 118MPa$, $G_c^f = 5.7 J/m^2$, $\sigma_c^f = 410MPa$, $G_c^{int} = 0.5 J/m^2$, $\sigma_c^{int} = 20MPa$ can be seen in Figure 4 b). Another example with same loading conditions and values for matrix and interface, but with $G_c^f = 3.4 J/m^2$, $\sigma_c^f = 118MPa$ is depicted in Figure 4 c). The crack paths have been received stepwise according to the cracking criterion. In this way, the full complexity of crack propagation, including crack branching and bridging can be captured. For energy

calculations Γ_C has to be considered as separated into disjoint parts Γ_i , $i = 1, \dots, n$, $n \in \mathbb{N}$. The fracture energy at the end of the simulation has to be calculated as sum over all distributions of the single crack pieces. For each crack Γ_i again the possibilities considered above can be thought of for increasing the fracture energy E_d . However, for a systematic study, we will have to return to a compromise scenario, in which the crack has exactly two options: to cross or to bypass the fibre.

CONCLUSION

We have considered the influence of different material parameters on the fracture energy for given load scenarios. It has been demonstrated that for the fibre breakage process the dissipated energy can be increased by adjusting the cohesive parameters of the fibre. It has also been shown that higher values of fracture energy for fibre debonding than for fibre breakage can be attained by adjusting geometrical parameters of the fibre. Additional to the studies for prescribed crack paths, simulation results have been shown for free crack propagation due to a stress criterion. The model reproduces complex cracking phenomena such as crack branching and bridging. The two approaches considering prescribed crack paths and free crack paths can be seen as limit cases. For future studies a middle way will be chosen, by permitting both the two prescribed crack paths of Figure 2. This will allow a systematic study of material parameters which lead either to fibre debonding or fibre breakage. Also the application of optimization tools for finding optimal material parameters and crack control is advisable. Possible directions for the controlling of crack growth can be found in [11].

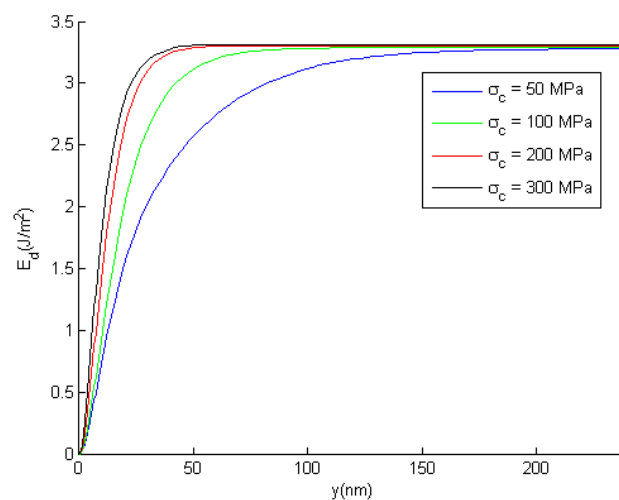


Figure 3. E_d for increased σ_c^{int}

ACKNOWLEDGEMENTS

The authors gratefully acknowledge the funding of the German Research Council (DFG), which, within the framework of its 'Excellence Initiative' supports the Cluster of Excellence ['Engineering of Advanced Materials'](#) at the University of Erlangen-Nuremberg. RJ thanks Steffen Brinckmann for insightful discussions.

REFERENCES

1. Needleman, A. (1987) *J. Appl. Mech.* **54**(233), 525-531.
2. Walter, M. E., Ravichandran, G., Ortiz, M. (1997) *Computational Mechanics* **20**, 192-198.
3. Geissler, G., Kaliske, M. (2003) *LACER* **8**, 281-296.
4. Nitsche, J. U. (1970) *Abhandlungen aus dem Mathematischen der Universität Hamburg* **36**, 9-15.
5. Mergheim, J., Kuhl, E., Steinmann, P. (2004) *Commun. Numer. Meth. Engng* **20**, 511-519.
6. Chandra, N., Li, A., Shet, C., Ghonem, H. (2002) *International Journal of Solids and Structures* **39**, 2827-2855.
7. Rose, J. H., Smith, J. R., Ferrante, J. (1983) *Phys. Rev. B* **28**, 1835 - 1845.
8. Ruiz, G., Ortiz, M., Pandolfi, A. (2000) *Int. J. Numer. Meth. Engng* **48**, 963-994.
9. Fritz, A., Hüeber, S., Wohlmuth, B. I. (2004) *CALCOLO* **41**, 115-137.
10. Nguyen, O., Ortiz, M. (2002) *Journal of the Mechanics and Physics of Solids* **50**, 1727-1741.
11. Khludnev, A., Leugering, G. (2009) *Preprint-Series of the Institute of Applied Mathematics*, Preprint No. 327, University of Erlangen-Nuremberg.

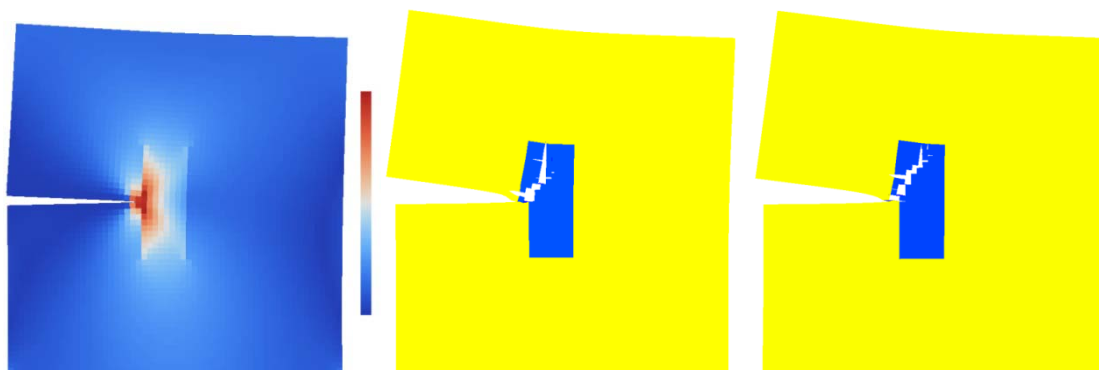


Figure 4. a) Stress distribution for incipient crack b) Crack path 1 c) Crack path 2